



Sea Surface Infrared Radiance Simulator

Part 1: Roughness and Temperature models of the Sea Surface Radiance

*Vivian Issa
Zahir A. Daya*

Defence R&D Canada – Atlantic

Technical Memorandum
DRDC Atlantic TM 2010-280
December 2010

This page intentionally left blank.

Sea Surface Infrared Radiance Simulator

Part 1: Roughness and Temperature models of the Sea Surface Radiance

Vivian Issa

Zahir A. Daya

Defence R&D Canada – Atlantic

Defence R&D Canada – Atlantic

Technical Memorandum

DRDC Atlantic TM 2010-280

December 2010

Principal Author

Original signed by Vivian Issa

Vivian Issa

Approved by

Original signed by Dave Hopkin

Dave Hopkin
Head/Maritime Asset Protection

Approved for release by

Original signed by Ron Kuwahara for

Calvin Hyatt
Head/Document Review Panel

- © Her Majesty the Queen in Right of Canada as represented by the Minister of National Defence, 2010
- © Sa Majesté la Reine (en droit du Canada), telle que représentée par le ministre de la Défense nationale, 2010

Abstract

This manuscript is the first in a sequence of documents that describe the development and verification of the various components of a sea surface infrared radiance simulator. We have developed an approach to modeling the sea surface radiance in the infrared to include both a coherent ship wake structure and an averaged background component. In this manuscript we discuss the component of the simulator for the ambient sea surface. The contribution from the background sea surface is determined by its roughness and temperature given a defined incident sky radiation. The roughness is largely determined by the wind speed at the sea surface and is described as a probability distribution of slopes of planar facets in the model. Then given the reflectivity and emissivity of the sea surface and their inherent dependencies on angle to the observer, temperature, and roughness we calculate the infrared radiance from the sea surface. We have illustrated the range of behaviour of the sea surface radiance for simple sky radiances at grazing and non-grazing angles as a function of sea roughness and temperature.

Résumé

Ce rapport est le premier d'une série de documents qui décrivent le développement et la vérification de plusieurs composantes d'un simulateur de la radiance de la surface de l'eau dans l'infrarouge. Nous avons développé une approche pour modéliser la radiance de la surface de l'eau dans l'infrarouge incluant, la fois, la contribution moyenne de l'arrière-plan maritime ainsi qu'une structure cohérente de sillages de navires. Dans le présent document, nous traitons la composante du simulateur qui concerne la contribution de la radiance de la surface de l'eau de l'arrière-plan maritime. Cette radiance émise par la surface de l'eau est déterminée principalement par sa température et sa rugosité. La rugosité de la surface de l'eau dépend largement de la vitesse du vent à sa surface. Elle est décrite par une fonction de densité de distribution de probabilité des pentes des différentes facettes planaires qui représentent la surface de l'eau dans le modèle. Ainsi, connaissant l'émissivité et la réflectivité de la surface de l'eau, leur dépendance avec l'angle de l'observateur, la température de l'eau et sa rugosité, nous avons calculé la radiance émise dans l'infrarouge de la surface de l'eau et celle qui y est réfléchie d'un ciel donnée. Nous avons illustré la dépendance du comportement de la radiance de la surface de l'eau pour différents angles d'observateur en fonction de la rugosité et de la température de la surface de l'eau en utilisant un modèle simplifié de la radiance du ciel.

This page intentionally left blank.

Executive summary

Sea Surface Infrared Radiance Simulator: Part 1: Roughness and Temperature models of the Sea Surface Radiance

Vivian Issa, Zahir A. Daya; DRDC Atlantic TM 2010-280; Defence R&D Canada – Atlantic; December 2010.

Background: Images, and the data extractable from them, are an indispensable component of a modern defence analysis capability. In the maritime domain, the sea surface which is seldom stationary, has a broad range of appearances in the visible and infrared optical bands. The optical appearance of the sea surface is influenced by wind, sky and clouds so much so that the basic measureables such as brightness or contrast vary significantly with prevailing and changing conditions. This sensitive dependence may be exacerbated in the infrared where the sea surface and the atmosphere are themselves thermal sources. There are several approaches to modeling the sea surface and its optical appearance visually and in the infrared, however, given the perpetual motion and inherent stochasticity of the sea surface, the measureables are invariably temporal or spatial averages. Yet there are often deterministic or long-lived coherent features on the sea surface such as ship wakes, swells and gravity waves. Ship wakes, in particular, are important features in airborne and satellite-based surveillance and are speculated to be a defence vulnerability.

Principal results: We have developed an approach to modeling the sea surface radiance in the infrared to include both a coherent ship wake structure and an averaged background component. The ship wake structure will consist, geometrically, of a Kelvin gravity wave field, a white water wake and a turbulent trailing wake. The background component derives from the probabilistic description of slopes of the sea surface due to the wind. Combining the sky and atmospheric radiation that is reflected by these features on the sea surface with the emitted radiation from the water and the radiation along the path, we can model the total radiance received by the observer. In brief, our sea surface simulator will consist of modular components for the ambient sea surface, for the ship wake, for the sky radiance and for the extended source to finite receiver geometry. At the present time, we discuss the component of the simulator for the ambient sea surface.

Significance: We have built a tool to simulate the reflected and emitted radiance from the sea surface knowing its temperature and geometry. This tool is a fundamental step for the study of the ships wakes radiance. Wakes are important because they are signatures rich in information and they persist on the surface of the water over several kilometers, and for several minutes. This importance is even more pronounced in the infrared because the sea surface and sky are thermal sources.

Future work: This manuscript is the first in a sequence of documents that describe the development and verification of the various components of our sea surface infrared radiance simulator. Subsequent manuscripts will describe the discretization and mapping of the sea surface to the observer's receiver optics, the geometrical and infrared models for the ship wake and the performance of the simulator.

Sommaire

Sea Surface Infrared Radiance Simulator: Part 1: Roughness and Temperature models of the Sea Surface Radiance

Vivian Issa, Zahir A. Daya ; DRDC Atlantic TM 2010-280 ; R & D pour la défense
Canada – Atlantique ; décembre 2010.

Contexte : Les images ainsi que les données que l'on peut extraire d'elles sont des éléments indispensables pour les analyses de la défense moderne. Dans le domaine maritime, la surface de l'eau, qui est rarement stationnaire, a une grande gamme d'apparences dans les bandes optiques du visible et de l'infrarouge. Le vent, le ciel et les nuages influencent grandement l'apparence optique de la surface de l'eau d'où la grande dépendance des quantités mesurables, telles que la brillance et le contraste, avec ces paramètres. Cette dépendance est accentuée dans l'infrarouge où le ciel et la surface de l'eau sont des sources thermiques. Il existe plusieurs approches pour modéliser la surface de l'eau et son apparence optique dans le visible et dans l'infrarouge. Étant donnée le mouvement perpétuel et stochastique de la surface de l'eau, ces variables sont moyennement constant temporellement et spatialement. Toutefois, la surface de l'eau peut avoir des traits cohérentes déterministes ou d'une durée plus longue tels que les sillages des navires, la houle et les vagues de gravités. Particulièrement, les sillages des bateaux, sont des traits importants pour la surveillance satellite et aérienne, ce qui est d'une grande importance pour les applications de la défense.

Résultats principaux : Nous avons développé une approche pour modéliser la radiance de la surface de l'eau dans l'infrarouge pour inclure à la fois l'arrière plan maritime et les sillages des navires. La structure du sillage est géométriquement constituée d'une onde de gravité de Kelvin, d'un sillage d'écume (zone d'eau blanche) et du sillage turbulent. L'arrière plan maritime est affecté par la vitesse du vent. Cette dernière est un paramètre important dans la fonction de distribution de densité de probabilité des pentes des facettes de la surface de l'eau. La radiance du ciel et de l'atmosphère réfléchi sur ces facettes ainsi que la radiance intrinsèque émise par ces mêmes facettes sont les deux composantes de la radiance reçue par un observateur. Bref, pour une géométrie spécifique de la source et de l'observateur, notre simulateur de la radiance de la surface de l'eau va contenir plusieurs composantes, soient la radiance de la surface de l'eau ambiante, celle de sillages de navires ainsi que celle de la radiance du ciel. Présentement, nous traitons la composante de la radiance de la surface de l'eau ambiante.

Importance : Nous avons un outil pour simuler la radiance réfléchi et émise par la surface de l'eau sachant sa température et sa géométrie. Cet outil est fondamentale pour l'étude de

sillages des navires. Les sillages des navires sont des signatures importantes puisqu'elles sont riches en informations et persistent sur la surface de l'eau sur plusieurs kilomètres et pour plusieurs minutes. Cette importance est encore plus prononcée dans l'infrarouge puisque le ciel et la surface de l'eau sont des sources thermiques.

Recherches futures : Ce document est le premier d'une série de documents qui décrivent le développement et la vérification de plusieurs composantes d'un simulateur infrarouge de la radiance de la surface de l'eau. Des documents ultérieurs suivront pour décrire le modèle de discrétisation de l'espace géométrique, le modèle infrarouge de sillages des navires ainsi que la performance du simulateur.

Table of contents

Abstract	i
Résumé	i
Executive summary	iii
Sommaire	v
Table of contents	vii
List of figures	viii
List of tables	viii
1 Introduction	1
2 Nomenclature	2
3 Framework for the Sea Surface Infrared Radiance Simulator	2
4 Sea Surface Roughness and Reflectivity	5
5 Sea Surface Emissivity	9
6 Results and Discussion	10
7 Conclusion and Future Work	12
References	20

List of figures

Figure 1:	A flowchart of the Sea Surface Infrared Radiance Simulator.	3
Figure 2:	The co-ordinate system and the geometry of a sea surface facet.	5
Figure 3:	The orientation of the normal vector for a sea surface facet.	7
Figure 4:	Models for the sea surface roughness and radiance.	14
Figure 5:	The dependence of emissivity and reflectivity of the sea surface on the angle of incidence.	15
Figure 6:	Emitted, reflected and total sea surface radiance as a function of the zenith angle.	16
Figure 7:	Dependence of the sea surface radiance on sea surface roughness for grazing angles.	17
Figure 8:	Dependence of the sea surface radiance on sea surface roughness for non-grazing angles.	18
Figure 9:	Dependence of the sea surface radiance on water temperature.	19

List of tables

Table 1:	Nomenclature of some radiation parameters.	2
Table 2:	The index of refraction of water for infrared light.	11

1 Introduction

Images, and the data extractable from them, are an indispensable component of a modern defence analysis capability. In the maritime domain, the sea surface which is seldom stationary, has a broad range of appearances in the visible and infrared optical bands. The optical appearance of the sea surface is influenced by wind, sky and clouds so much so that the basic measureables such as brightness or contrast vary significantly with prevailing and changing conditions. This sensitive dependence may be exacerbated in the infrared where the sea surface and the atmosphere are themselves thermal sources.

The sea surface is complex: the surface is not constant, it is not always mathematically smooth having cusps and singularities when it is rough, it extends to the limits of visibility, its appearance depends on the position of the observer (the viewing angle from the average normal to the sea surface) reflecting different parts of the sky which can be clear or cloudy etc. There are several approaches to modeling the sea surface and its optical appearance visually and in the infrared [1, 2, 3, 4, 5], however, given the perpetual motion and inherent stochasticity of the sea surface, the measureables are invariably temporal or spatial averages. Yet there are often deterministic or long-lived coherent features on the sea surface such as ship wakes, swells and gravity waves. Ship wakes, in particular, are important features in airborne and satellite-based surveillance (see *e.g.* [6]) and are speculated to be a defence vulnerability.

Our approach to modeling the sea surface radiance in the infrared is designed to include both a coherent ship wake structure and an averaged background component. The ship wake structure will consist, geometrically, of a Kelvin gravity wave field, a white water wake and a turbulent trailing wake. The background component derives from the probabilistic description of slopes of the sea surface due to the wind. Combining the sky and atmospheric radiation that is reflected by these features on the sea surface with the emitted radiation from the water and the radiation along the path, we can model the total radiance received by the observer. Whereas, this general ‘summation of different parts’ approach appears simple in principle, its implementation is rife with intricacies, some of which are discussed in Section 3. In brief, our sea surface simulator will consist of modular components for the ambient sea surface, for the ship wake, for the sky radiance and for the extended source to finite receiver geometry.

This manuscript is the first in a sequence of documents that describe the development and verification of the various components of our sea surface infrared radiance simulator. In this manuscript, we briefly describe the overall framework (Section 3) and the module for the infrared radiance from the ambient or background sea surface. This module accounts for the reflected infrared radiance from the sky (Section 4) and for thermally emitted infrared radiance from the water (Section 5). Results of the numerically computed infrared radiance as a function of sea surface roughness, temperature and viewing angle are discussed in Section 6 which is followed by a short conclusion in Section 7. Subsequent manuscripts

will describe the discretization and mapping of the sea surface to the observer's receiver optics, the geometrical and infrared models for the ship wake and the performance of the simulator.

2 Nomenclature

Radiation theory is a mature field in which has emerged a nomenclature that facilitates a precise description of the physical quantity juxtaposed with the interaction geometry. In Table 1 we have described a few of the more commonly used radiation parameters that we use in our development of the sea surface radiance model. In particular we will require the incident radiation on the sea surface from the sky, the reflected radiation and the emitted radiation to model the total radiance of the sea surface.

Symbol	Quantity	Description	Units (SI)
U	Radiant energy	Energy traveling in the form of EM waves	J
Φ	Radiant flux	Time rate of flow of radiant energy	W
M	Emittance, Exitance	Radiant flux emitted per unit area of the radiating source	W/m^2
E	Irradiance	Total radiant flux incident on a surface per unit area of the irradiated surface per unit of solid angle around the irradiative surface	W/m^2
I	Radiant Intensity	Total radiant flux per unit of solid angle around the radiating source	W/sr
L	Radiance, Stere-radiance, Specific intensity, Brightness	The rate of energy radiation (radiant flux) from a source per unit of solid angle and per unit of area of the source	$W/(sr.m^2)$

Table 1: Nomenclature of some radiation parameters.

3 Framework for the Sea Surface Infrared Radiance Simulator

Calculating the infrared radiance received by an observer from the sea surface is a methodical process which in our simulator consists of four modules. These describe the ambient or background sea surface, the sea surface disturbed by the ship wake, the sky infrared radiance incident on the sea surface, and the receiver-source geometry. In Figure 1 we

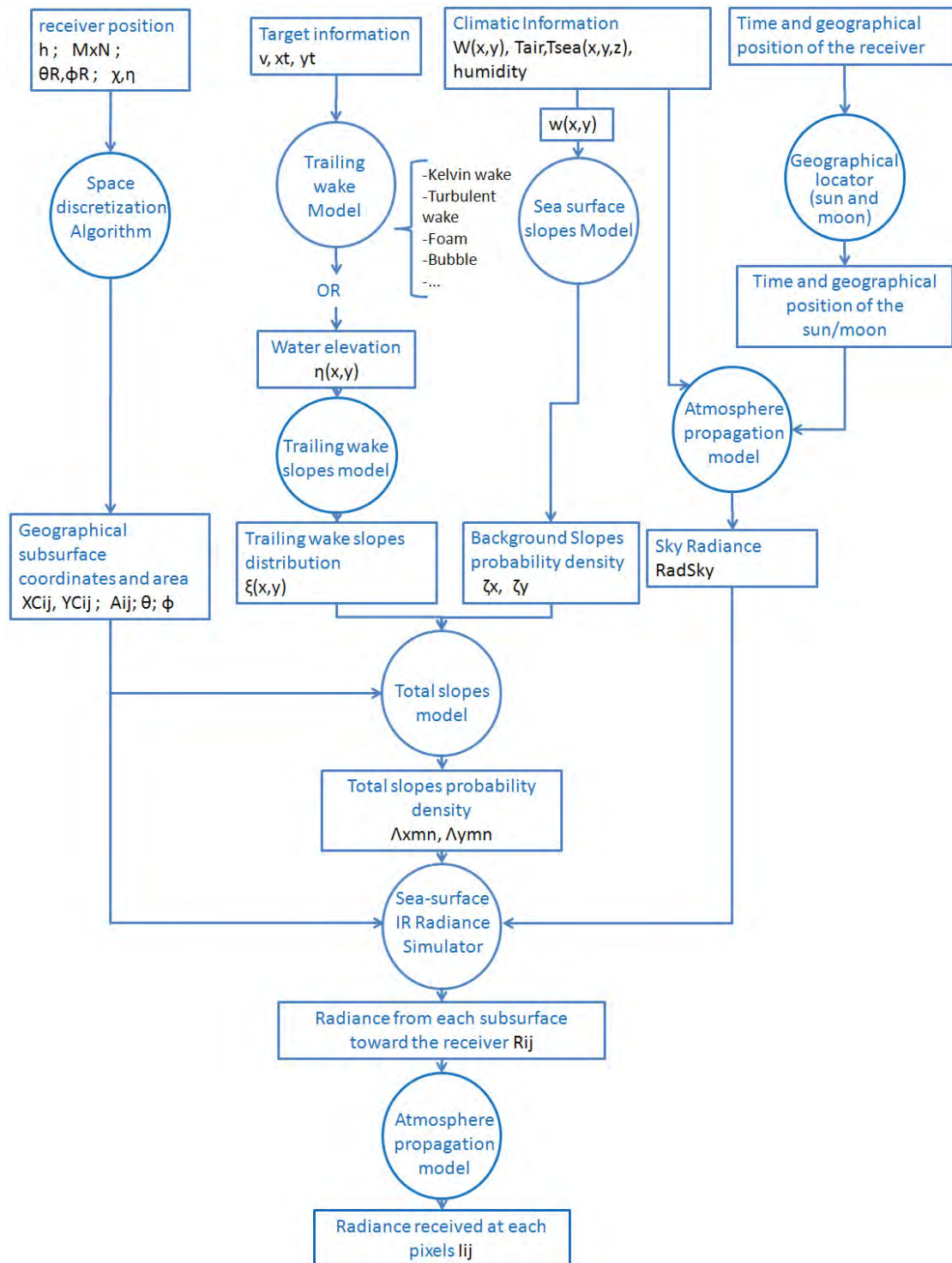


Figure 1: A flowchart of the Sea Surface Infrared Radiance Simulator.

have illustrated the procedure that is implemented in our simulator to compute the infrared radiance at each pixel of the receiver from the appropriate patch of sea surface. In the flowchart, circles correspond to algorithms while rectangles denote input or output data. In total, there are eight algorithms of which only two will be described in this paper.

The contribution from the background sea surface is determined by its roughness and temperature given a defined incident sky radiation. The roughness is largely determined by the wind speed at the sea surface and is generally described as a probability distribution of slopes of facets or patches of the surface. The temperature will vary with season and the underlying ocean currents that vary geographically. Then given the reflectivity and emissivity of the sea surface and their inherent dependencies on angle to the observer, temperature, and roughness we can calculate the infrared radiance from the sea surface. These elements are described in detail in Sections 4 and 5.

A ship wake imprints onto the sea surface a distinct ‘V’ shaped pattern. Within the ‘V’ shape, the roughness of the sea surface is significantly modified, while outside, the background sea surface persists. With distance downstream from the ship the ‘V’ fades with the background sea gradually infringing upon the wake until it vanishes. The wake consists of the Kelvin gravity waves, some white water wake along the ship and astern, and a trailing wake consisting of a turbulent bubbly water [7]. The gravity waves introduce a smooth undulation on the sea surface, while the white water is a result of the surface breaking up and entraining air. The trailing wake can have roughness that is significantly different from the background sea and its reflectivity is thus different [8, 9]. Additionally, if a thermal stratification is disturbed by the ship, the trailing wake can be thermally different from the undisturbed background sea surface [10]. See Reference [11] for an introduction to various elements of a ship wake in the infrared. In our simulator, we will develop a model for the ship wake roughness and ship wake temperature which will be published in a subsequent paper.

In addition to the emitted radiation from the sea, infrared radiation from the sky which is incident on the sea surface is also reflected toward the observer. The sky, from an observer’s point of view, consists of the integrated effect of infrared emitters between the observer and space. This includes the celestial sources such as stars, the moon and in particular the sun, as well as clouds and other emissions from atmospheric molecular components. There are several models for skylight from clear skies [12, 13], whereas, cloudy skies are usually modeled with the MODTRAN atmospheric propagation model [14, 15]. In our simulator, we expect to integrate existing models for sky radiation that is incident on the sea surface. In a future paper, we will describe the choice of sky model and its implementation.

The receiver–source geometry model will accurately map a discrete facet of the sea surface to a pixel in the receiving element. The mismatch between the sea surface which is an extended source on a curved earth and a rectangular pixel at the receiver results in a non-trivial discretization of the sea surface in the numerical calculations. These will be

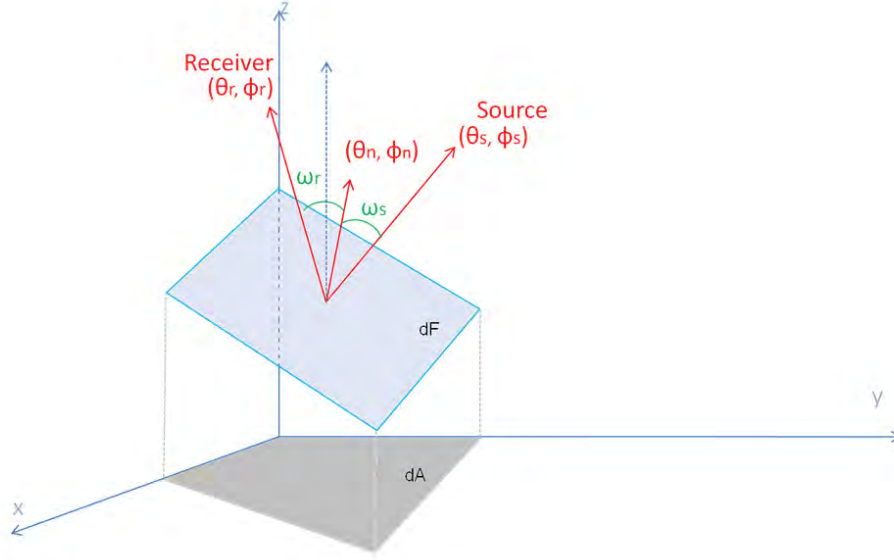


Figure 2: The co-ordinate system and the geometry of a sea surface facet.

discussed in a subsequent manuscript. With these four modules, we intend to develop an infrared sea surface radiance simulator capable of modeling the infrared radiance of a ship wake.

4 Sea Surface Roughness and Reflectivity

In modeling the sea surface, we consider it to be tessellated by planar facets. The facet geometry, shown in Figure 2, is the basic element of the sea surface for which we will calculate the reflected and emitted radiances. Planar facets will fully cover the sea surface with each facet approximating the orientation of the local sea surface up to the first order derivative or slope in two dimensions.

In order to define the sea surface model we require a distribution of facet slopes that is representative of the real sea. There are several experimental measurements and therefore experimentally-derived models of the distribution of sea surface slopes under various wind-driven sea states *e.g.* the Cox & Munk model [5], the Shaw-Churnside model [16] etc. In this development we will use the Cox & Munk (CM) model, however, we are able to implement other sea surface models. The CM model for the probability of a facet with slope z_x and z_y when the sea surface is driven by a wind of speed w m/s is given by

$$p(z_x, z_y, w) \approx \frac{1}{2\pi\sigma_u\sigma_c} \exp \left[-\frac{1}{2} \left(\frac{z_x^2}{\sigma_u^2} + \frac{z_y^2}{\sigma_c^2} \right) \right], \quad (1)$$

where

$$\begin{aligned}\sigma_u^2 &= 3.16 \times 10^{-3}w \\ \sigma_c^2 &= 0.003 + 1.92 \times 10^{-3}w\end{aligned}\tag{2}$$

In Eq 1, z_x is the slope of the facet in upwind direction while z_y is the slope in crosswind direction. The mean value of the slopes is zero while their variances in the upwind and crosswind directions are σ_u^2 and σ_c^2 , respectively.

To calculate the total radiance received at the receiver from a facet, we must account for the reflected and emitted components. Below we address the reflected part while the emitted component is described in Section 5. The reflected radiance at the receiver from a facet depends on the reflectivity of the facet in the direction of the receiver and on the incident radiance from the part of the source that can, by geometry, be reflected to the receiver. As shown in Figure 2 the normal to the facet and the directions to the receiver and source are in standard spherical co-ordinates with polar or zenith angle θ and azimuthal angle ϕ . Simple geometry demands that specular reflection off the facet with normal (θ_n, ϕ_n) that is received at a receiver in the direction (θ_r, ϕ_r) must originate from the source at (θ_s, ϕ_s) such that the angle of incidence ω_s equals the angle of reflection ω_r .

In our model, the direction of the observer or receiver (θ_r, ϕ_r) and the slopes of the facet (z_x, z_y) are known. The directions of the facet normal (θ_n, ϕ_n) and the source (θ_s, ϕ_s) have to be expressed in terms of these known parameters. A little algebra gives

$$\theta_n = \text{atan}\left(\sqrt{z_x^2 + z_y^2}\right),\tag{3}$$

and

$$\phi_n = \begin{cases} \text{atan}\left(\frac{z_y}{z_x}\right) & z_x < 0 \text{ and } z_y < 0, \\ \text{atan}\left(\frac{z_y}{z_x}\right) + 2\pi & z_x < 0 \text{ and } z_y > 0, \\ \text{atan}\left(\frac{z_y}{z_x}\right) + \pi & z_x > 0. \end{cases}\tag{4}$$

In Figure 3 we have plotted the orientations of the facet normal vector $\hat{n} = (\theta_n, \phi_n)$ for the range of different slopes. Equations 3 and 4 express the direction of the facet normal (θ_n, ϕ_n) in terms of the presumed facet slopes z_x and z_y .

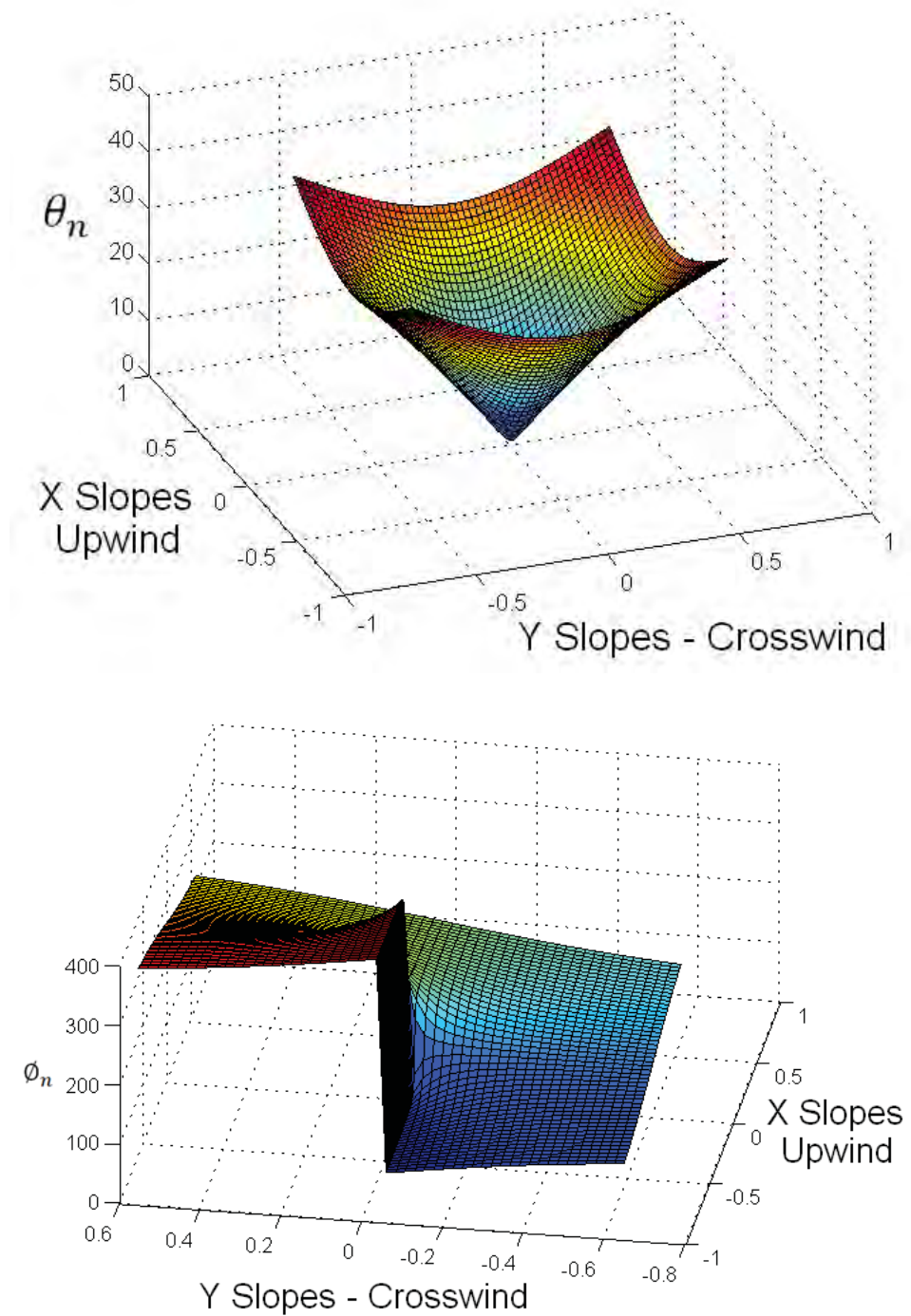


Figure 3: The orientation of the normal vector $\hat{n} = (\theta_n, \phi_n)$ for a sea surface facet as a function of the slopes z_x and z_y .

The part of the sky source that is reflected toward the receiver is determined by $\omega_s = \omega_r = \omega$. Note that since \hat{n}, \hat{s} and \hat{r} (the unit vectors for the facet normal, source and receiver) are in the same plane we find that

$$\cos\theta_s = 2\zeta\cos\theta_n - \cos\theta_r, \quad (5)$$

and

$$\cos\phi_s = 2\zeta\sin\theta_n\cos\phi_n - \sin\theta_r\cos\phi_r\sin\theta_s, \quad (6)$$

where

$$\zeta = \sin\theta_n\cos\phi_n\sin\theta_r\cos\phi_r + \sin\theta_n\sin\phi_n\sin\theta_r\sin\phi_r + \cos\theta_n\cos\theta_r = \hat{n} \cdot \hat{r} = \cos\omega \quad (7)$$

Equations 5–7 express the orientation of the vector to the part of the sky that is reflected by a facet with slope (z_x, z_y) toward a receiver at (θ_r, ϕ_r) . This completes the basic geometric relations for calculating the reflected component.

We denote the sky or source radiance incident on a facet from the direction (θ_s, ϕ_s) to be L_s . Then the reflected radiance in the direction of the receiver $L_r(\theta_s, \phi_s)$ is given by

$$L_r(\theta_r, \phi_r) = \rho(\theta_r, \phi_r) \times L_s(\theta_s, \phi_s), \quad (8)$$

where the $\rho(\theta_r, \phi_r)$ is the reflectivity (reflectance) in the direction of the receiver. We specify the reflectivity of the sea water surface in Section 6. Equation 8 is a local relation for the incident radiation reflected toward a receiver by a single facet. In contrast, a pixel at the receiver will likely sample an area of sea surface that is composed of many facets. Therefore, the reflected radiance at the receiving pixel will be the additive contribution of the reflection off many facets. In fact we will assume that the number of facets is sufficiently numerous so that their slopes are distributed according to the Cox & Munk probability function of Eq. 1. We denote the horizontal projection of the area of all facets with slope $(z_x \pm dz_x, z_y \pm dz_y)$ by dA_h (See Fig. 2 for a schematic for a single facet). Adding the area projections over all the facets that are visible to the receiver pixel we obtain the total horizontally projected area A_h . Then the ratio

$$\frac{dA_h}{A_h} = p(z_x, z_y) dz_x dz_y, \quad (9)$$

is the fractional occurrence of facets with slopes $(z_x \pm dz_x, z_y \pm dz_y)$ that are viewed by the receiver pixel. From this basic relation, it follows that

$$\frac{dA_n}{A_h} = \frac{1}{\cos\theta_n} p(z_x, z_y) dz_x dz_y, \quad (10)$$

and

$$\frac{dA_r}{A_h} = \frac{\cos\omega_r}{\cos\theta_n} p(z_x, z_y) dz_x dz_y, \quad (11)$$

which is the same relationship but expressed in terms of area projections on the facet normal and toward the receiver. Denoting by A_r the total area projected by the facets toward the receiver we have

$$\frac{dA_r}{A_r} = \frac{A_h \cos\omega_r}{A_r \cos\theta_n} p(z_x, z_y) dz_x dz_y. \quad (12)$$

Equation 8 describes the contribution to the reflected radiance from the sky to the receiver from a single facet with slope (z_x, z_y) while Eq. 12 defines the area weight with which facets with slopes $(z_x \pm dz_x, z_y \pm dz_y)$ are projected toward the receiver. Then it follows that the reflected radiance at the receiver pixel is given by

$$dL_r(\theta_r, \phi_r) = \rho(\theta_r, \phi_r) \times L_s(\theta_s, \phi_s) \times \frac{A_h \cos\omega_r}{A_r \cos\theta_n} p(z_x, z_y) dz_x dz_y. \quad (13)$$

Note that when $\omega_r > 90$, the facet is pointing away from detector. So, only slopes with $\omega_r \leq 90$ should be considered.

Finally, with $p_0 = \underbrace{\int \int \frac{A_h \cos\omega_r}{A_r \cos\theta_n} p(z_x, z_y) dz_x dz_y}_{\omega \leq \frac{\pi}{2}}$ as a normalisation factor for the probability

distribution function, the total reflected radiance arriving at a single pixel at receiver is then the sum over all slopes:

$$L_r(\theta_r, \phi_r) = \frac{1}{p_0} \underbrace{\int \int}_{\omega \leq \frac{\pi}{2}} \rho(\theta_r, \phi_r) \times L_s(\theta_s, \phi_s) \times \frac{A_h \cos\omega_r}{A_r \cos\theta_n} p(z_x, z_y) dz_x dz_y. \quad (14)$$

5 Sea Surface Emissivity

The derivation of the total emitted radiation from the sea surface that is received is similar to that in Section 4. From a single facet, the infrared radiation emitted toward a receiver in the direction (θ_r, ϕ_r) is given by

$$L_e(\theta_r, \phi_r) = \varepsilon(\theta_r, \phi_r) \frac{P(T, \lambda)}{\pi}, \quad (15)$$

with

$$P(T, \lambda) = \frac{2\pi hc^2}{\lambda^5 (e^{\frac{ch}{k\lambda T}} - 1)}, \quad (16)$$

where $\varepsilon(\theta_r, \phi_r) = 1 - \rho(\theta_r, \phi_r)$ is the emissivity and $P(T, \lambda)$ is the Planck black body function at temperature T (c , h , and k are physical constants for the speed of light, Planck's constant and Boltzmann constant).

A pixel at the receiver is radiated by many facets with the different slopes. Once again Eq. 12 quantifies the area weight projected toward the receiver of the facets with slopes $(z_x \pm dz_x, z_y \pm dz_y)$. It follows that the emitted radiation received from these facets is

$$dL_e(\theta_r, \phi_r) = [1 - \rho(\theta_r, \phi_r)] \times \frac{P(T, \lambda)}{\pi} \times \frac{A_h \cos \omega_r}{A_r \cos \theta_n} p(z_x, z_y) dz_x dz_y. \quad (17)$$

The total emitted radiance at a receiver pixel is given by integrating over all slopes:

$$L_e(\theta_r, \phi_r) = \frac{1}{p_0} \underbrace{\int \int}_{\omega \leq \frac{\pi}{2}} [1 - \rho(\theta_r, \phi_r)] \times \frac{P(T, \lambda)}{\pi} \times \frac{A_h \cos \omega_r}{A_r \cos \theta_n} p(z_x, z_y) dz_x dz_y. \quad (18)$$

6 Results and Discussion

Our principal result is the total radiance at a receiver pixel from a patch of sea surface that is comprised of many facets. The total radiance is the sum of the reflected (Eq. 14) and emitted (Eq. 18) contributions:

$$\begin{aligned} L(\theta_r, \phi_r) &= L_e(\theta_r, \phi_r) + L_r(\theta_r, \phi_r) \\ &= \frac{1}{p_0} \underbrace{\int \int}_{\omega \leq \frac{\pi}{2}} \left\{ [1 - \rho(\theta_r, \phi_r)] \times \frac{P(T, \lambda)}{\pi} \right. \\ &\quad \left. + \rho(\theta_r, \phi_r) \times L_s(\theta_s, \phi_s) \right\} \times \frac{A_h \cos \omega_r}{A_r \cos \theta_n} p(z_x, z_y) dz_x dz_y \end{aligned} \quad (19)$$

This radiance model for the Cox & Munk sea surface is comparable to several others that are currently used in the scientific community, see Fig. 4 for a short list.

In calculating Eq. 19, we map a patch of sea surface to a receiver pixel given the instantaneous field of view of the pixel and the viewing position and orientation. The patch of sea surface is covered by a collection of facets whose slopes are sampled from the Cox & Munk probability distribution. For each patch we determine the orientation toward the receiver and then compute the emitted and reflected radiation. For these we need to specify the emissivity or reflectivity $\rho(\theta_r, \phi_r)$ for the sea water facet and the incident sky radiation $L_s(\theta_s, \phi_s)$. The reflectance can be determined from the index of refraction of water by the Fresnel equations. In Table 2 we have listed the index of refraction of seawater for infrared radiation of wavelength $3.4 - 5.2\mu\text{m}$ at 25°C from Hale & Querry [17]. The resulting reflectivity and emissivity are independent of ϕ_r and vary with the zenith angle θ_r as shown in Fig. 5. When viewed from directly overhead ($\theta_r = 0$), the sea surface is essentially emissive with near-vanishing reflectance, while at grazing angles ($\theta_r \approx 90^\circ$) the sea surface is primarily reflective with near-vanishing emissivity. The strong variation of the reflectance with zenith angle is expected to significantly impact the total radiance at the receiver.

λ [m]	$n(\lambda)$	λ [m]	$n(\lambda)$	λ [m]	$n(\lambda)$	λ [m]	$n(\lambda)$
3.4	1.42	3.9	1.357	4.4	1.334	4.9	1.328
3.5	1.4	4	1.351	4.5	1.332	5	1.325
3.6	1.385	4.1	1.346	4.6	1.330	5.1	1.322
3.7	1.374	4.2	1.342	4.7	1.330	5.2	1.317
3.8	1.364	4.3	1.338	4.8	1.330	5.3	1.312

Table 2: The index of refraction of water for infrared light at 25°C .

The sky radiance that is incident on a facet of the sea surface originates primarily from scattered sunlight and thermal emission from clouds and the atmosphere. Other stellar sources such as moon light are important on clear nights. Whereas the sky radiance is heterogeneous, for the purposes of demonstrating our simulator, we have chosen a sky radiance that is independent of the azimuthal and zenith angles. We illustrate two cases where the constant sky radiance is greater or less than the thermal emission from the sea surface. Given the sky radiance and the reflectance function, we can calculate the total radiance at the receiver for a given sea temperature and sea surface roughness.

In Fig. 6 we have plotted the emitted, reflected and total sea surface radiance at the receiver for a sky radiance that is greater and lesser than the emitted sea radiance. We find that the total radiance increases with the zenith angle generally following the shape of the reflected sea surface radiance which is increasingly important at grazing angles. When the sky radiance is lower than the intrinsic sea surface radiance, the total radiance decreases with the zenith angle generally following the shape of the intrinsic sea surface radiance. As

noted earlier, these behaviours stem from the dependence of the emissivity and reflectance on the zenith angle as determined by the Fresnel equations.

At constant temperature, the variation of the reflected radiance with sea roughness determines the variation of the total sea radiance. In Fig. 7 we have plotted the total radiance received as a function of wind speed, effectively sea surface roughness, for a zenith angle of 75° for an incident sky radiance that exceeds the emitted sea surface radiance. At grazing angles, the angle between the receiver and the normal to the facets decreases with increasing roughness. This is equivalent to, on average, a lower reflectivity and a higher emissivity. Consequently, when the sky radiance is greater (lesser) than the emitted sea surface radiance, the total sea surface radiance increases (decreases) with roughness. At non-grazing angles, the angle between the receiver and the normal to the facets increase with roughness. On average, this amounts to an increase in reflectivity and a decrease in emissivity. Consequently, when the sky radiance is greater (lesser) than the emitted sea surface radiance, the total sea surface radiance increases (decreases) with roughness as shown in Fig. 8.

In contrast to the variation of sea surface radiance with roughness, the dependence of the emitted radiation on sea surface temperature is monotonic: in Fig. 9, we have illustrated this behaviour for grazing and non-grazing angles and for sky radiances greater than and lesser than the sea surface radiance.

7 Conclusion and Future Work

In this manuscript we have described the framework and development of a sea surface radiance simulator that is envisioned to account for the effects of optically coherent structures, particularly ship wakes on the sea surface, as well as the pseudo-random wind driven sea surface. Our approach is designed to utilize existing third party modules for modeling the radiance from the sky, atmosphere and propagation of infrared radiation. At this time we have described the model for the background sea surface. It consists of a wind driven surface that can be locally approximated by planar facets defining spatial gradients in the upwind and crosswind directions. The orientation of the facets or more directly the slopes that determine the orientation are sampled from an empirical probability distribution. With well defined reflectance and emissivity for sea water, we modeled the reflected sky radiance and the emitted black body radiance by the sea surface. With our simulation we have illustrated the dependence of the sea surface radiance on roughness and temperature which serve to verify the functioning of the background sea surface simulator.

Subsequent manuscripts will describe three other modules that interface with the background module described here. A sky radiance model based on third party software ShipIR and atmospheric propagation software MODTRAN will be incorporated to take into account realistic distributions of sky radiance from solar scattering, non-uniform cloud cover,

aerosols and stellar radiation. A home-grown model mapping the extended sea surface to a receiver will be published. The model describes the receiver optics relating the signal received at a single pixel to the patch of sea surface that is imaged, and the subsequent discretization of the patch into a collection of planar facets. And finally, a module for the ship wake is under development. The model will account for the various features of a ship wake taking into account the undulation of the sea surface due to the Kelvin gravity waves, the damped-capillary waves in the trailing wake, the thermal wake in stratified waters and the white water wake. The capability to accurately model, in the optical and infrared bands, a ship wake in the background sea is at present a significant deficiency in the infrared sea and target modeling community.

	Slopes model	Sea surface radiance model	Used approximations And notes
Schwartz and Priest (6)	$p(\theta, \phi) \approx \frac{1}{2\pi ab} \tan \theta \sec^2 \theta \exp[-\tan^2 \theta A(\phi)]$ <p>With</p> $A(\phi) = \frac{1}{2} \left(\frac{\cos^2 \phi}{a^2} + \frac{\sin^2 \phi}{b^2} \right)$	<p>Used $\hat{f}(\theta, \phi)$ the fractional LOS projected area to weight the facet contribution to the radiance</p> $R_a(\hat{\theta}) = \int_0^{\pi/2} d\theta \int_0^{2\pi} d\phi \hat{f}(\theta, \phi) \{ [1 - \rho(\Omega)] R_B + \rho(\Omega) R_s(\theta') \}$	Only the isotropic case is considered: $a^2 = b^2 = \sigma^2$ $= 0.003 + 0.00512 W$
Zeisse (3)	<p>Cox & Munk :</p> $p(\zeta_x, \zeta_y, W) \approx \frac{1}{2\pi\sigma_u\sigma_c} \exp \left[-\frac{1}{2} \left(\frac{\zeta_x^2}{\sigma_u^2} + \frac{\zeta_y^2}{\sigma_c^2} \right) \right]$ $\sigma_u^2 = 3.16 \times 10^{-3} W$ $\sigma_c^2 = 0.003 + 1.92 \times 10^{-3} W$	$\int \{ [1 - \rho(\theta_r, \phi_r)] * P(T, \lambda) + \rho(\theta_r, \phi_r) * I_s(\theta_s, \phi_s) \} * \frac{A \cos \omega_r}{B \cos \theta_n} p(z_x, z_y) dz_x dz_y$	
Wu and Smith (7)	$p(\zeta_x, \zeta_y, W) \approx \frac{1}{2\pi\sigma^2} \exp \left[-\frac{1}{2\sigma^2} (\zeta_x^2 + \zeta_y^2) \right]$ $2\sigma^2 = 0.003 + 0.00512 W$ <p>That is C&M in the isotropic case.</p>		Isotropic case
Monzon and al. (8)	<p>C&M :</p> $p(\zeta_x, \zeta_y, W) \approx \frac{1}{2\pi\sigma_u\sigma_c} \exp \left[-\frac{1}{2} \left(\frac{\zeta_x^2}{\sigma_u^2} + \frac{\zeta_y^2}{\sigma_c^2} \right) \right]$ $\sigma_u^2 = 3.16 \times 10^{-3} W$ $\sigma_c^2 = 0.003 + 1.92 \times 10^{-3} W$	<p>Following Zeisse's derivation:</p> $N(\theta, \phi) = \frac{1}{4C(\theta, \phi)} \iint_{\text{sky}} \rho(\omega) N^{\text{inc}}(\theta', \phi') \times p(x, y) (1 + x^2 + y^2)^2 d\Omega'$	Ignored: Sea emissivity, Sky reflection, Path radiance. Solar disc effects are considered only.

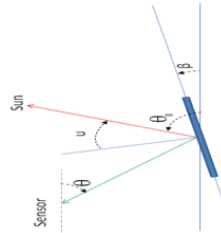


Figure 4: Models for the sea surface roughness and radiance.

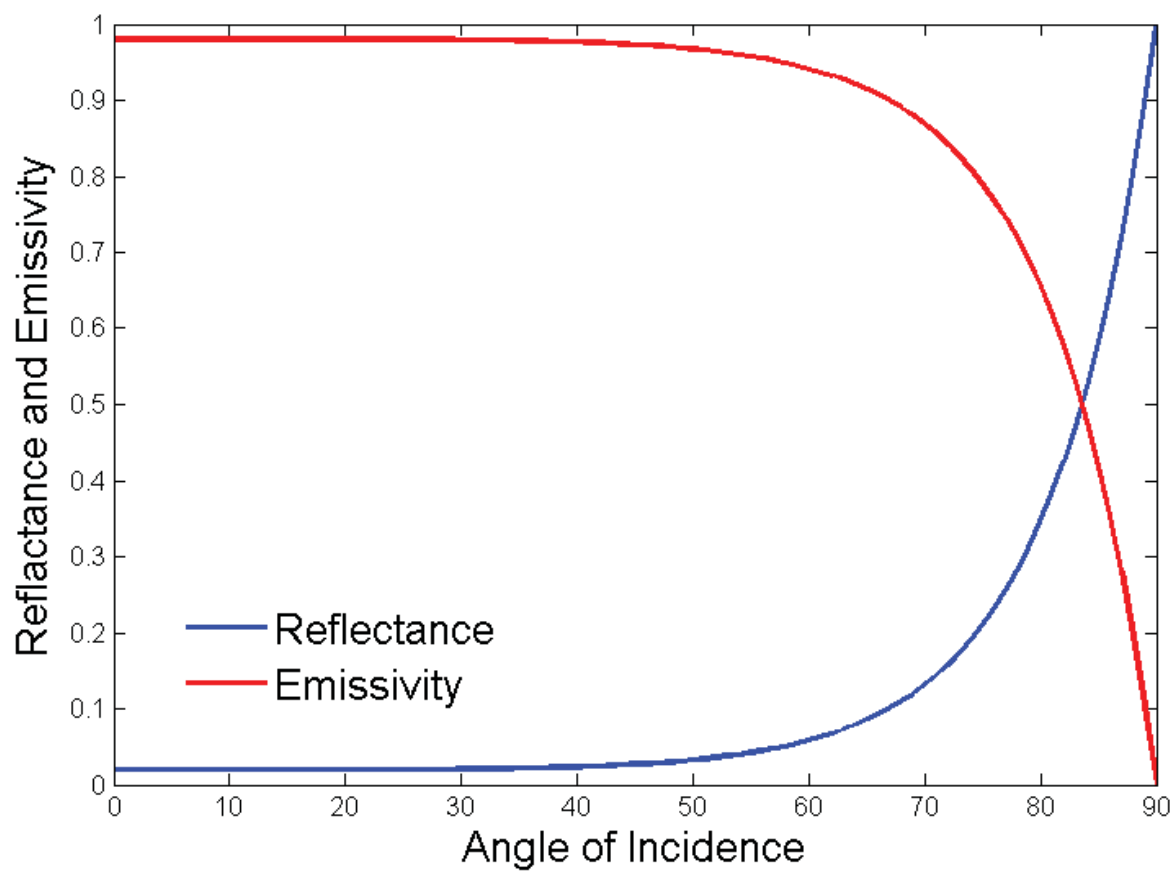


Figure 5: The dependence of emissivity and reflectivity of the sea surface on the angle of incidence.

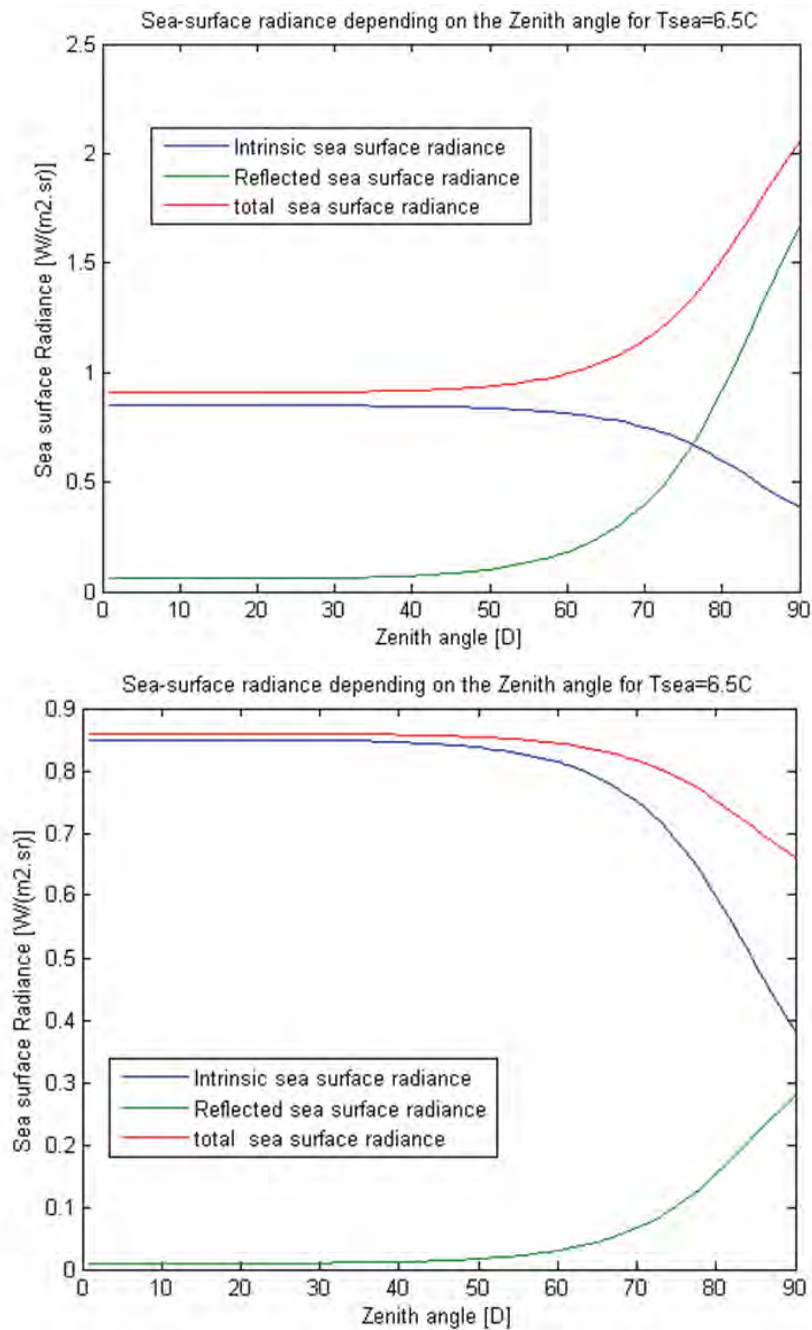


Figure 6: The emitted, reflected and total sea surface radiance as a function of the zenith angle for a uniform sky with sky radiance greater than the emitted sea surface radiance (top) and sky radiance less than the emitted sea surface radiance (bottom).

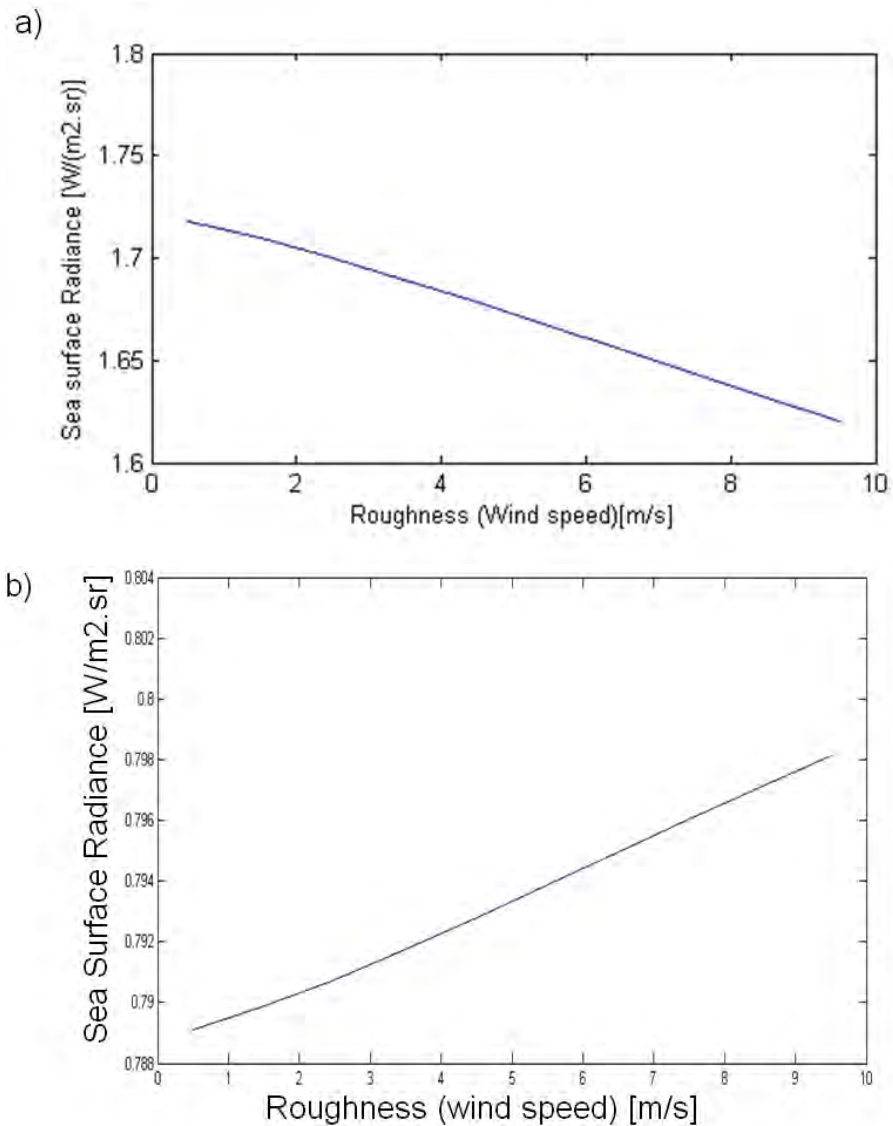


Figure 7: The dependence of the sea surface radiance on sea surface roughness for a zenith angle of 75° with (a) constant sky radiance greater than the emitted sea radiance and (b) constant sky radiance lesser than the emitted sea radiance.

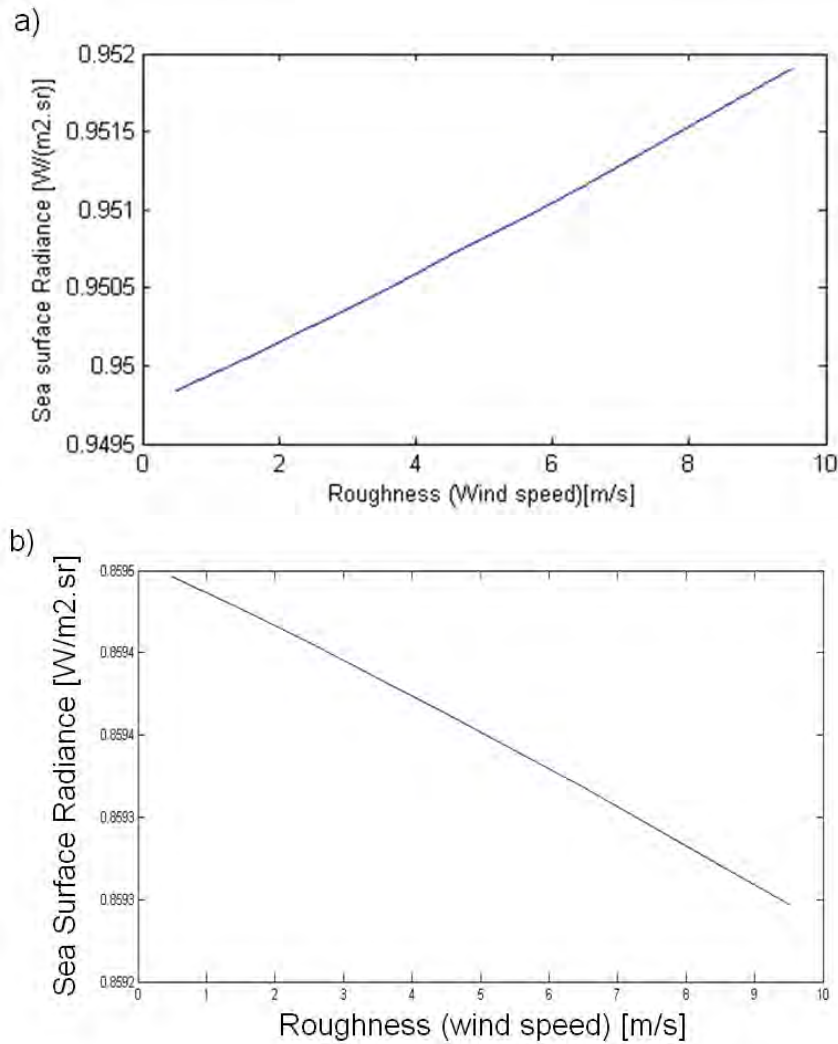


Figure 8: The dependence of the sea surface radiance on sea surface roughness for a zenith angle of 25° with (a) constant sky radiance greater than the emitted sea radiance and (b) constant sky radiance lesser than the emitted sea radiance.

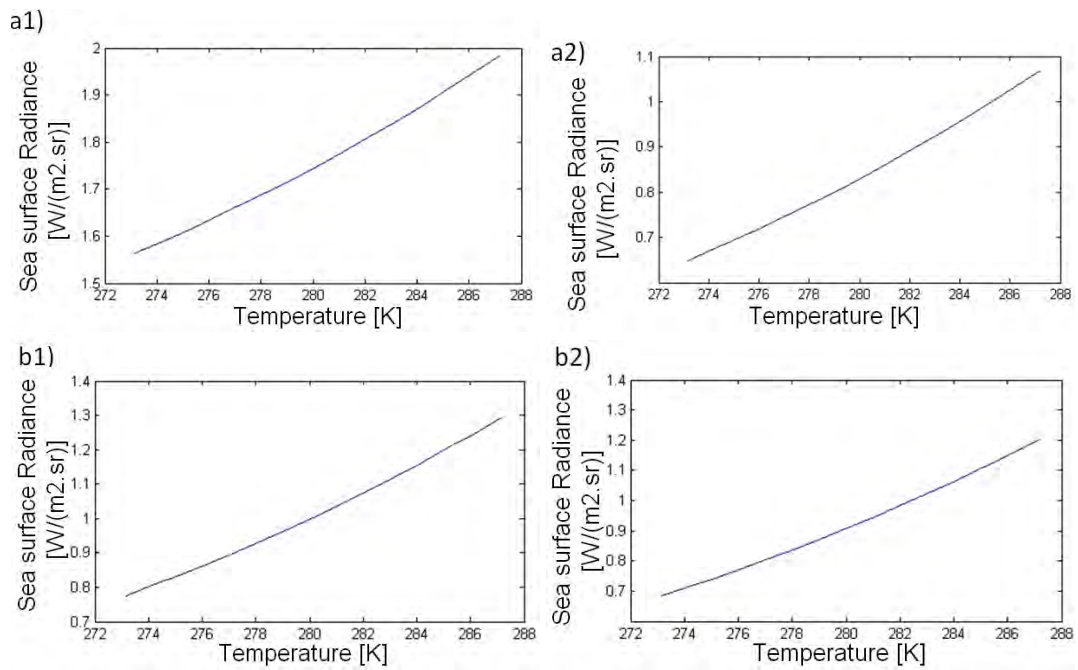


Figure 9: The dependence of the sea surface radiance on the water temperature for a uniform sky with: a1) sky radiance greater than the emitted sea surface radiance for a high zenith angle; b1) for a low zenith angle; a2) sky radiance lesser than the intrinsic sea surface radiance for a high zenith angle; b2) for a low zenith angle.

References

- [1] C. R. Zeisse, C. P. McGrath, K. M. Littfin and H. G. Hughes. Infrared radiance of the wind-ruffled sea. *Journal of the Optical Society of America A*, Vol. 16, pp 1439–1452, 1999.
- [2] C. R. Zeisse. Radiance of the Ocean Horizon. *Journal of the Optical Society of America*, Vol. 12, pp 2022, 1995.
- [3] X. Wu and W. L. Smith. Emissivity of rough sea surface for 8 – 13 μ m: modelling and verification. *Applied Optics*, Vol. 36(12), pp 2609–2619, 1997.
- [4] C. Monzon, D.W. Forester, R. Burkhart and J. Bellemare. Rough ocean surface and sunlint region characteristics. *Journal of the Optical Society of America A*, Vol. 45, pp 7089, 2006.
- [5] C. Cox and W. Munk. Measurement of the Roughness of the Sea Surface from Photographs of the sun Glitter. *Journal of the Optical Society of America*, Vol. 44, pp 838, 1954.
- [6] G. Zilman, A. Zapolski, and M. Marom. The Speed and Beam of a Ship From Its Wake's SAR Images. *IEEE Transactions on Geoscience and Remote Sensing*, Vol. 42(10), pp 2335–2343, 2004.
- [7] R. D. Peltzer, W. D. Garrett, and P. M. Smith. A remote sensing study of a surface ship wake. *Int. J. Remote Sensing*, Vol. 8(5), pp 689–704, 1987.
- [8] Z. A. Daya and C. Galloway. Infrared intensity of the trailing turbulent surface wake of CFAV QUEST in trial Q300. *DRDC Atlantic TM*, TM 2010–175, 2010.
- [9] I. B. Schwartz and R. G. Priest. Reflection driven ship wake contrasts in the infrared. *NRL Report 9144*, 1988.
- [10] M. Stewart. Numerical Prediction of Thermal Ship Wakes. *NRL Memorandum Report 5955*, 1987.
- [11] Z. A. Daya and D. L. Hutt. Rudiments of Ship Wakes in the Infrared. *DRDC Atlantic Technical Memorandum*, TM 2010–168, 2010.
- [12] H. E. Bennett, J. M. Bennett, and M. R. Nagel. Distribution of Infrared Radiance over a Clear Sky. *Journal of the Optical Society of America*, Vol. 50(2): pp 100–106, 1960.
- [13] S. B. Idso and R. D. Jackson. Thermal Radiation from the Atmosphere. *Journal of Geophysical Research*, Vol. 38(15), pp 5397–5403, 1969.

- [14] H. G. Hughes and C. R. Zeisse. Infrared Propagation Modeling beneath Marine Stratus Clouds. *Journal Of Atmospheric And Oceanic Technology*, Vol. 17, pp 504–511, 2000.
- [15] E. J. Lentilucci. Using MODTRAN Predicting Sensor-Reaching Radiance. *Chester F. Carlson Center for Imaging Science and Rochester Institute of Technology*, 2007.
- [16] J.A. Shaw and J.H. Churnside. Scanning-laser glint measurements of sea-surface slope statistics. *Appl. Opt. (USA)*, Vol. 36, pp 4202 - 13, 1997.
- [17] G. M. Hale and M. R. Querry. Optical constants of water in the 200 nm to 200 μm wavelength Region. *Applied Optics*, Vol. 12, pp 555, 1973.

This page intentionally left blank.

Distribution list

DRDC Atlantic TM 2010-280

Internal distribution

- 1 Author
- 1 Co-author
- 1 SH/MAP
- 3 Library

Total internal copies: 6

External distribution

Department of National Defence

- 1 DRDKIM
NDHQ/DRDKIM

Other Canadian recipients

- 1 David A. Vaitekunas
Senior Development Engineer
W.R. Davis Engineering Ltd
1260 Old Innes Road
Ottawa, Ontario
CANADA K1B 3V3
- 1 Library and Archives Canada
Attn: Military Archivist, Government Records Branch

International recipients

- 1 Douglas Fraedrich
Naval Research Laboratory
Attn: Code 5757
4555 Overlook Ave., SW
Washington, DC 20375-5339 USA

Total external copies: 4

Total copies: 10

This page intentionally left blank.

DOCUMENT CONTROL DATA		
(Security classification of title, body of abstract and indexing annotation must be entered when document is classified)		
1. ORIGINATOR (The name and address of the organization preparing the document. Organizations for whom the document was prepared, e.g. Centre sponsoring a contractor's report, or tasking agency, are entered in section 8.) Defence R&D Canada – Atlantic PO Box 1012, Dartmouth NS B2Y 3Z7, Canada	2. SECURITY CLASSIFICATION (Overall security classification of the document including special warning terms if applicable.) UNCLASSIFIED	
3. TITLE (The complete document title as indicated on the title page. Its classification should be indicated by the appropriate abbreviation (S, C or U) in parentheses after the title.) Sea Surface Infrared Radiance Simulator: Part 1: Roughness and Temperature models of the Sea Surface Radiance		
4. AUTHORS (Last name, followed by initials – ranks, titles, etc. not to be used.) Issa, V.; Daya, Z. A.		
5. DATE OF PUBLICATION (Month and year of publication of document.) December 2010	6a. NO. OF PAGES (Total containing information. Include Annexes, Appendices, etc.) 36	6b. NO. OF REFS (Total cited in document.) 17
7. DESCRIPTIVE NOTES (The category of the document, e.g. technical report, technical note or memorandum. If appropriate, enter the type of report, e.g. interim, progress, summary, annual or final. Give the inclusive dates when a specific reporting period is covered.) Technical Memorandum		
8. SPONSORING ACTIVITY (The name of the department project office or laboratory sponsoring the research and development – include address.) Defence R&D Canada – Atlantic PO Box 1012, Dartmouth NS B2Y 3Z7, Canada		
9a. PROJECT OR GRANT NO. (If appropriate, the applicable research and development project or grant number under which the document was written. Please specify whether project or grant.) 11gf	9b. CONTRACT NO. (If appropriate, the applicable number under which the document was written.)	
10a. ORIGINATOR'S DOCUMENT NUMBER (The official document number by which the document is identified by the originating activity. This number must be unique to this document.) DRDC Atlantic TM 2010-280	10b. OTHER DOCUMENT NO(s). (Any other numbers which may be assigned this document either by the originator or by the sponsor.)	
11. DOCUMENT AVAILABILITY (Any limitations on further dissemination of the document, other than those imposed by security classification.) (X) Unlimited distribution () Defence departments and defence contractors; further distribution only as approved () Defence departments and Canadian defence contractors; further distribution only as approved () Government departments and agencies; further distribution only as approved () Defence departments; further distribution only as approved () Other (please specify):		
12. DOCUMENT ANNOUNCEMENT (Any limitation to the bibliographic announcement of this document. This will normally correspond to the Document Availability (11). However, where further distribution (beyond the audience specified in (11)) is possible, a wider announcement audience may be selected.)		

13. ABSTRACT (A brief and factual summary of the document. It may also appear elsewhere in the body of the document itself. It is highly desirable that the abstract of classified documents be unclassified. Each paragraph of the abstract shall begin with an indication of the security classification of the information in the paragraph (unless the document itself is unclassified) represented as (S), (C), or (U). It is not necessary to include here abstracts in both official languages unless the text is bilingual.)

This manuscript is the first in a sequence of documents that describe the development and verification of the various components of a sea surface infrared radiance simulator. We have developed an approach to modeling the sea surface radiance in the infrared to include both a coherent ship wake structure and an averaged background component. In this manuscript we discuss the component of the simulator for the ambient sea surface. The contribution from the background sea surface is determined by its roughness and temperature given a defined incident sky radiation. The roughness is largely determined by the wind speed at the sea surface and is described as a probability distribution of slopes of planar facets in the model. Then given the reflectivity and emissivity of the sea surface and their inherent dependencies on angle to the observer, temperature, and roughness we calculate the infrared radiance from the sea surface. We have illustrated the range of behaviour of the sea surface radiance for simple sky radiances at grazing and non-grazing angles as a function of sea roughness and temperature.

14. KEYWORDS, DESCRIPTORS or IDENTIFIERS (Technically meaningful terms or short phrases that characterize a document and could be helpful in cataloguing the document. They should be selected so that no security classification is required. Identifiers, such as equipment model designation, trade name, military project code name, geographic location may also be included. If possible keywords should be selected from a published thesaurus. e.g. Thesaurus of Engineering and Scientific Terms (TEST) and that thesaurus identified. If it is not possible to select indexing terms which are Unclassified, the classification of each should be indicated as with the title.)

sea surface reflectivity
sea surface emissivity
sea surface roughness
infrared sea radiance

This page intentionally left blank.

Defence R&D Canada

Canada's leader in defence
and National Security
Science and Technology

R & D pour la défense Canada

Chef de file au Canada en matière
de science et de technologie pour
la défense et la sécurité nationale



www.drdc-rddc.gc.ca